

# Top flavour-changing neutral interactions: theoretical expectations and experimental detection \*

J. A. Aguilar–Saavedra

*Departamento de Física and CFTP,  
Instituto Superior Técnico, P-1049-001 Lisboa, Portugal*

## Abstract

Top flavour-changing neutral interactions with a light quark  $q = u, c$  and a gauge or Higgs boson are very suppressed within the Standard Model (SM), but can reach observable levels in many of its extensions. We review the possible size of the effective vertices  $Ztq$ ,  $\gamma tq$ ,  $gtq$  and  $Htq$  in several SM extensions, and discuss the processes in which these interactions might show up at LHC and at a high energy  $e^+e^-$  linear collider.

## 1 Introduction

The next generation of high energy colliders planned or under construction will test the Standard Model (SM) with high precision and will explore higher energies in the search of new physics. New physics may manifest itself in two ways: through direct signals involving the production of new particles or by departures from the SM predictions for the known particles. Direct signals are crucial in order to establish the type of new physics present in nature but indirect effects are important as well, and in some cases they could give evidence of physics beyond the SM before new particles are discovered.

The top quark plays a key role in the quest for deviations from SM predictions for two reasons: (*i*) due to its large mass, radiative corrections involving new particles are often more important than for lighter fermions; (*ii*) its large mass suggests that it might have a special role in electroweak symmetry breaking. Top quarks will be copiously produced at LHC and, to a lesser extent, at a high energy  $e^+e^-$  collider like TESLA. With such large samples, precise measurements of its couplings will be

---

\*Presented at the final meeting of the European Network “Physics at Colliders”, Montpellier, September 26-27, 2004.

available to test SM predictions [1, 2]. Here we study flavour-changing neutral (FCN) couplings involving the top quark. The most general effective Lagrangian describing its interactions with a light quark  $q = u, c$  and a gauge or Higgs boson, containing terms up to dimension 5, can be written as

$$\begin{aligned}
-\mathcal{L}^{\text{eff}} = & \frac{g}{2c_W} X_{qt} \bar{q} \gamma_\mu (x_{qt}^L P_L + x_{qt}^R P_R) t Z^\mu + \frac{g}{2c_W} \kappa_{qt} \bar{q} (\kappa_{qt}^v + \kappa_{qt}^a \gamma_5) \frac{i\sigma_{\mu\nu} q^\nu}{m_t} t Z^\mu \\
& + e \lambda_{qt} \bar{q} (\lambda_{qt}^v + \lambda_{qt}^a \gamma_5) \frac{i\sigma_{\mu\nu} q^\nu}{m_t} t A^\mu + g_s \zeta_{qt} \bar{q} (\zeta_{qt}^v + \zeta_{qt}^a \gamma_5) \frac{i\sigma_{\mu\nu} q^\nu}{m_t} T^a q G^{a\mu} \\
& + \frac{g}{2\sqrt{2}} g_{qt} \bar{q} (g_{qt}^v + g_{qt}^a \gamma_5) t H + \text{H.c.}, \tag{1}
\end{aligned}$$

where  $q^\nu = (p_t - p_q)^\nu$  is the boson momentum and  $\bar{q}, t$  are shorthands for the quark fields  $\bar{u}(p_q)$  and  $u(p_t)$ , respectively. The couplings are constants corresponding to the first terms in the expansion in momenta, normalised to  $|x_{qt}^L|^2 + |x_{qt}^R|^2 = 1$ ,  $|\kappa_{qt}^v|^2 + |\kappa_{qt}^a|^2 = 1$ , etc., with  $X_{qt}, \kappa_{qt}, \lambda_{qt}, \zeta_{qt}$  and  $g_{qt}$  real and positive. In principle there are additional terms that could be included in this effective Lagrangian, for instance proportional to  $\sigma_{\mu\nu}(p_t + p_q)^\nu Z^\mu$ . However, in the processes discussed the top quark can be considered on its mass shell to a very good approximation and the gauge bosons are either on their mass shell or coupling to light fermions. Hence, these extra interactions can be rewritten in terms of the ones in Eq. (1) using Gordon identities.

Within the SM, the  $\gamma_\mu$  couplings  $x_{qt}^{L,R}$  vanish at the tree level by the GIM mechanism, and non-renormalisable  $\sigma_{\mu\nu}$  terms do not appear in the Lagrangian. Both types of vertices are generated at one loop level but, as will be shown in Section 2, they are strongly suppressed by the GIM mechanism, making FCN top interactions very small. In models beyond the SM this GIM suppression can be relaxed, and one-loop diagrams mediated by new bosons may also contribute, yielding effective couplings orders of magnitude larger than those of the SM. The possible size of top FCN vertices in several SM extensions will be summarised in Section 3. These interactions lead to various top decay and single top production processes which will be discussed in Section 4. The observation of such processes, extremely rare in the SM, would provide a clear indirect signal of new physics, although the presence of SM backgrounds must be considered. In specific models, the presence of these interactions may be correlated with other effects at high or low energies. One example of such correlation will be shown in Section 5.

We note that in the literature there are numerous alternative normalisations of the coupling constants in  $\mathcal{L}^{\text{eff}}$ . For this reason, we express our limits on the couplings in terms of top decay branching ratios. We use  $m_t = 178.0 \pm 4.3$  GeV [3],  $\alpha(m_t) =$

$1/128.921$ ,  $s_W^2(m_t) = 0.2342$ ,  $\alpha_s(m_t) = 0.108$  and assume  $m_H = 115$  GeV. The tree-level prediction for the leading decay mode  $t \rightarrow bW^+$  is

$$\Gamma(t \rightarrow bW^+) = \frac{\alpha}{16 s_W^2} |V_{tb}|^2 \frac{m_t^3}{M_W^2} \left[ 1 - 3 \frac{M_W^4}{m_t^4} + 2 \frac{M_W^6}{m_t^6} \right], \quad (2)$$

which yields  $\Gamma(t \rightarrow bW^+) = 1.61$  GeV. We take this value as the total top width  $\Gamma_t$ . The partial widths for FCN decays are given by

$$\begin{aligned} \Gamma(t \rightarrow qZ)_\gamma &= \frac{\alpha}{32 s_W^2 c_W^2} |X_{qt}|^2 \frac{m_t^3}{M_Z^2} \left[ 1 - \frac{M_Z^2}{m_t^2} \right]^2 \left[ 1 + 2 \frac{M_Z^2}{m_t^2} \right], \\ \Gamma(t \rightarrow qZ)_\sigma &= \frac{\alpha}{16 s_W^2 c_W^2} |\kappa_{qt}|^2 m_t \left[ 1 - \frac{M_Z^2}{m_t^2} \right]^2 \left[ 2 + \frac{M_Z^2}{m_t^2} \right], \\ \Gamma(t \rightarrow q\gamma) &= \frac{\alpha}{2} |\lambda_{qt}|^2 m_t, \\ \Gamma(t \rightarrow qg) &= \frac{2\alpha_s}{3} |\zeta_{qt}|^2 m_t, \\ \Gamma(t \rightarrow qH) &= \frac{\alpha}{32 s_W^2} |g_{qt}|^2 m_t \left[ 1 - \frac{M_H^2}{m_t^2} \right]^2. \end{aligned} \quad (3)$$

The corresponding branching ratios are then

$$\begin{aligned} \text{Br}(t \rightarrow qZ)_\gamma &= 0.472 X_{qt}^2, \\ \text{Br}(t \rightarrow qZ)_\sigma &= 0.367 \kappa_{qt}^2, \\ \text{Br}(t \rightarrow q\gamma) &= 0.428 \lambda_{qt}^2, \\ \text{Br}(t \rightarrow qg) &= 7.93 \zeta_{qt}^2, \\ \text{Br}(t \rightarrow qH) &= 3.88 \times 10^{-2} g_{qt}^2. \end{aligned} \quad (4)$$

## 2 Top FCN interactions in the SM

One-loop induced FCN couplings involving the top quark have a strong GIM suppression, resulting in negligible branching ratios for top FCN decays [4, 5]. We show how this cancellation mechanism operates taking as example the  $\gamma tc$  vertex. The SM diagrams contributing at one loop level are depicted in Fig. 1, with  $d_i = d, s, b$ . We omit the diagrams involving unphysical scalars, which can be obtained replacing the  $W$  boson lines by charged scalars.

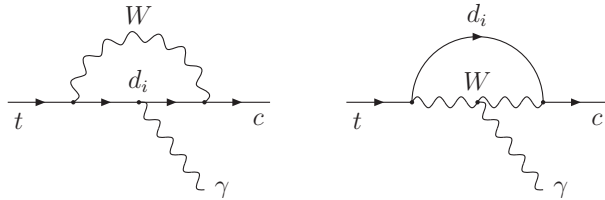


Figure 1: SM diagrams contributing to the  $tc\gamma$  vertex. The additional diagrams involving unphysical scalars are not displayed.

If we define  $\mathcal{V}_\gamma \equiv e\lambda_{qt}\lambda_{qt}^v/m_t$ ,  $\mathcal{A}_\gamma \equiv e\lambda_{qt}\lambda_{qt}^a/m_t$ , we can write these form factors as

$$\begin{aligned}\mathcal{V}_\gamma &= \sum_{i=1}^3 f_{\gamma V}(m_i^2/M_W^2)V_{ci}V_{ti}^*, \\ \mathcal{A}_\gamma &= \sum_{i=1}^3 f_{\gamma A}(m_i^2/M_W^2)V_{ci}V_{ti}^*,\end{aligned}\tag{5}$$

with  $f_{\gamma V}(x) \simeq f_{\gamma A}(x)$  (equal in the limit  $m_c = 0$ ) and  $V$  the Cabibbo-Kobayashi-Maskawa (CKM) matrix. The function  $f_{\gamma V}$  is shown in Fig. 2 (a). Using the fact that  $m_{d,s} \simeq 0$  to an excellent approximation, the  $3 \times 3$  CKM unitarity relation  $V_{cd}V_{td}^* + V_{cs}V_{ts}^* + V_{cb}V_{tb}^* = 0$  implies

$$\mathcal{V}_\gamma = [f_{\gamma V}(m_b^2/M_W^2) - f_{\gamma V}(0)]V_{cb}V_{tb}^* \equiv f'_{\gamma V}(m_b^2/M_W^2)V_{cb}V_{tb}^*.\tag{6}$$

Hence, the form factor is controlled by the shifted function  $f'_{\gamma V}$ , plotted in Fig. 2 (b). We observe that the consequence of  $3 \times 3$  CKM unitarity is to cancel the constant term  $f_{\gamma V}(0) \simeq -5.1 \times 10^{-6} - 6.0 \times 10^{-6}i$ , common to the three  $d, s, b$  contributions, leaving  $\mathcal{V}_\gamma$  proportional to the much smaller function  $f'_{\gamma V}(m_b^2/M_W^2) \simeq f'_{\gamma V}(0.0012) \simeq -9.1 \times 10^{-9} - 4.7 \times 10^{-9}i$ .

This cancellation makes the form factors rather sensitive to the value of the  $b$  quark mass in the internal propagators. The most adequate choice is the running  $\overline{\text{MS}}$  mass evaluated at a scale  $O(m_t)$ . With  $\overline{m}_b(m_t) = 2.74 \pm 0.17$  GeV, the SM prediction for  $t \rightarrow c\gamma$  is [6]

$$\text{Br}(t \rightarrow c\gamma) = (4.6_{-1.0}^{+1.2} \pm 0.2 \pm 0.4_{-0.5}^{+1.6}) \times 10^{-14}.\tag{7}$$

The first and second uncertainties quoted come from the bottom and top masses, respectively, the third from CKM matrix elements and the fourth is estimated varying the renormalisation scale between  $M_Z$  (plus sign) and  $1.5 m_t$  (minus sign). The analogous calculation of  $t \rightarrow c\gamma$  yields

$$\text{Br}(t \rightarrow c\gamma) = (4.6_{-0.9}^{+1.1} \pm 0.2 \pm 0.4_{-0.7}^{+2.1}) \times 10^{-12}.\tag{8}$$

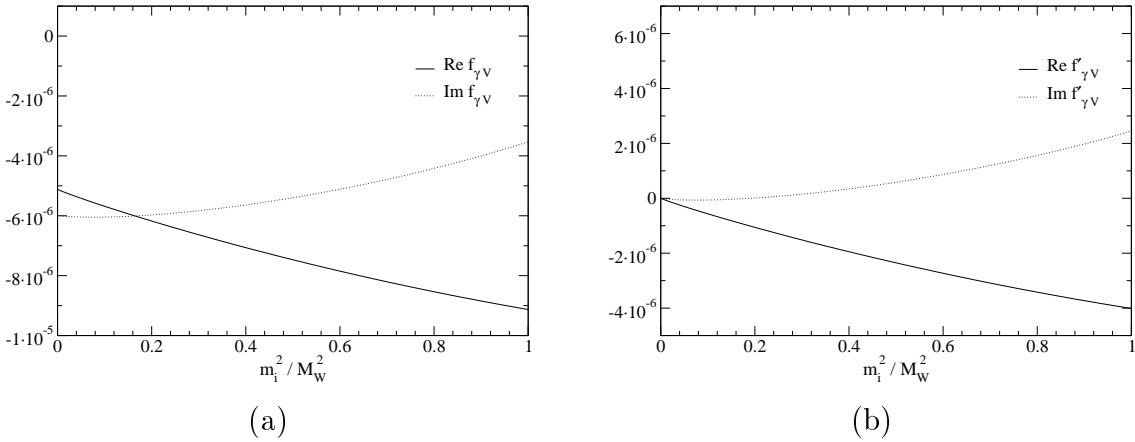


Figure 2: Loop functions  $f_{\gamma V}(m_i^2/M_W^2)$  and  $f'_{\gamma V}(m_i^2/M_W^2)$ .

These updated results are one order of magnitude smaller than the values previously obtained in Ref. [4]. For  $t \rightarrow cZ$ ,  $t \rightarrow cH$  the results of Refs. [4, 5] must be rescaled by a factor  $[\overline{m}_b(m_t)/(5 \text{ GeV})]^4 \simeq 0.09$  (the loop functions are approximately linear for  $m_b^2/M_W^2 \ll 1$ ), obtaining

$$\begin{aligned} \text{Br}(t \rightarrow cZ) &\simeq 1 \times 10^{-14}, \\ \text{Br}(t \rightarrow cH) &\simeq 3 \times 10^{-15}. \end{aligned} \quad (9)$$

The relative uncertainties on these values are expected to be similar to the ones in Eqs. (7),(8). For decays  $t \rightarrow uZ$ ,  $t \rightarrow u\gamma$ ,  $t \rightarrow ug$ ,  $t \rightarrow uH$  the branching ratios are a factor  $|V_{ub}/V_{cb}|^2 \simeq 0.0079$  smaller to the ones corresponding to a  $c$  quark, as can be seen from Eq. (6). The difference between the  $u$  and  $c$  masses is irrelevant.

### 3 Top FCN interactions beyond the SM

New physics contributions to the effective Lagrangian in Eq. (1) can enhance the rates of top FCN decays several orders of magnitude, giving observable branching ratios in some regions of parameter space. Here we examine the situation in the context of models with extra quark singlets, with an extra Higgs doublet and in supersymmetric extensions of the SM.

In models with extra quarks the  $3 \times 3$  CKM matrix is no longer unitary and the GIM mechanism acting to suppress the SM amplitudes is relaxed. When the new quarks are

$SU(2)_L$  singlets with charge  $Q = 2/3$ , the couplings of the  $Z$  boson to up-type quarks are not diagonal. Taking a conservative value for the mass of the new quark,  $m_T \geq 300$  GeV, present experimental data allow

$$X_{qt} \simeq 0.015 \quad (|x_{qt}^L| = 1, x_{qt}^R = 0) \quad (10)$$

at the tree level [7]. Such couplings are possible both for up and charm quarks, but not simultaneously. In these models there also exist tree-level FCN scalar interactions, given by

$$g_{qt} \simeq \frac{m_t}{M_W} X_{qt} \quad (g_{qt}^v = g_{qt}^a). \quad (11)$$

The branching ratios for top decays mediated by these vertices are  $\text{Br}(t \rightarrow qZ) \simeq 1.1 \times 10^{-4}$ ,  $\text{Br}(t \rightarrow qH) \simeq 4.1 \times 10^{-5}$ , respectively. The decay rates for  $t \rightarrow q\gamma$ ,  $t \rightarrow qg$  are also enhanced due to the partial breaking of  $3 \times 3$  CKM unitarity and the presence of extra Feynman diagrams like those in Fig. 1 (a) but with an  $u$  or  $t$  internal quark and a  $Z$  boson. The rates obtained are  $\text{Br}(t \rightarrow q\gamma) \simeq 7.5 \times 10^{-9}$ ,  $\text{Br}(t \rightarrow qg) \simeq 1.5 \times 10^{-7}$  for  $X_{qt} \simeq 0.015$ . In models with  $Q = -1/3$  singlets the branching ratios are much smaller [6] since CKM unitarity breaking is very constrained by experimental data. In SM extensions with  $SU(2)_L$  doublets there may also exist right-handed tree-level FCN couplings  $X_{qt}$  [8].

FCN interactions with scalars are also present at the tree level in two Higgs doublet models (2HDMs), unless a discrete symmetry is imposed to forbid them. The couplings are often assumed to scale with quark masses [9],

$$g_{qt} \simeq \frac{\sqrt{m_q m_t}}{M_W} \quad (12)$$

up to a factor of order unity, *i.e.*  $g_{ct} \simeq 0.20$ ,  $g_{ut} \simeq 0.012$ , leading to  $\text{Br}(t \rightarrow cH) \simeq 1.5 \times 10^{-3}$ ,  $\text{Br}(t \rightarrow uH) \simeq 5.5 \times 10^{-6}$ , respectively. The new scalar fields also give radiative contributions to the  $Ztq$ ,  $\gamma tq$  and  $gtq$  vertices, with diagrams analogous to those in Fig. 1, replacing the  $W$  boson by a charged scalar, and additional diagrams with an up-type internal quark and a neutral scalar. The resulting branching ratios can be up to  $\text{Br}(t \rightarrow cZ) \sim 10^{-7}$ ,  $\text{Br}(t \rightarrow c\gamma) \sim 10^{-6}$ ,  $\text{Br}(t \rightarrow cg) \sim 10^{-4}$  [10, 11], with smaller values for decays to an up quark. In 2HDMs without tree-level scalar FCN couplings, charged and neutral Higgs contributions to  $\mathcal{L}^{\text{eff}}$  can still increase significantly the rates for top FCN decays with respect to the SM predictions. The maximum values reached are of the order  $\text{Br}(t \rightarrow cZ) \sim 10^{-10}$ ,  $\text{Br}(t \rightarrow c\gamma) \sim 10^{-9}$ ,  $\text{Br}(t \rightarrow cg) \sim 10^{-8}$ ,  $\text{Br}(t \rightarrow cH) \sim 10^{-5}$  [11, 12].

Recent calculations in the context of the Minimal Supersymmetric Standard Model (MSSM) show that for non-universal squark mass terms  $\text{Br}(t \rightarrow qZ) \simeq 2 \times 10^{-6}$ ,  $\text{Br}(t \rightarrow q\gamma) \simeq 2 \times 10^{-6}$ ,  $\text{Br}(t \rightarrow qg) \simeq 10^{-4}$  can be reached while keeping agreement with low energy data [13, 14]. These results are larger than previous estimates [15–17]. The branching ratio of  $t \rightarrow qH$  can be up to  $\text{Br}(t \rightarrow qH) \sim 10^{-5}$  [18], assuming squark masses above 200 GeV. In all these decays the largest contributions to the amplitudes come from gluino exchange diagrams. In non-minimal supersymmetric models with  $R$  parity violation, top FCN decays can also proceed through baryon number violating interactions, yielding  $\text{Br}(t \rightarrow qZ) \simeq 3 \times 10^{-5}$ ,  $\text{Br}(t \rightarrow q\gamma) \simeq 1 \times 10^{-6}$ ,  $\text{Br}(t \rightarrow qg) \simeq 2 \times 10^{-4}$  [19],  $\text{Br}(t \rightarrow qH) \sim 10^{-6}$  [20]. (We obtain these values taking  $\Lambda = 1$  in Refs. [19, 20].)

We collect the data presented in this section in Table 1, together with SM predictions. Two conclusions can be extracted from these figures: (i) Models with tree-level FCN couplings to  $Z$ ,  $H$  give the largest rates for decays to these particles, as it is expected; (ii) the radiative decays  $t \rightarrow q\gamma$ ,  $t \rightarrow qg$  have largest branching ratios in supersymmetric extensions of the SM.

	SM	QS	2HDM	FC 2HDM	MSSM	$\mathcal{R}$ SUSY
$t \rightarrow uZ$	$8 \times 10^{-17}$	$1.1 \times 10^{-4}$	–	–	$2 \times 10^{-6}$	$3 \times 10^{-5}$
$t \rightarrow u\gamma$	$3.7 \times 10^{-16}$	$7.5 \times 10^{-9}$	–	–	$2 \times 10^{-6}$	$1 \times 10^{-6}$
$t \rightarrow ug$	$3.7 \times 10^{-14}$	$1.5 \times 10^{-7}$	–	–	$8 \times 10^{-5}$	$2 \times 10^{-4}$
$t \rightarrow uH$	$2 \times 10^{-17}$	$4.1 \times 10^{-5}$	$5.5 \times 10^{-6}$	–	$10^{-5}$	$\sim 10^{-6}$
$t \rightarrow cZ$	$1 \times 10^{-14}$	$1.1 \times 10^{-4}$	$\sim 10^{-7}$	$\sim 10^{-10}$	$2 \times 10^{-6}$	$3 \times 10^{-5}$
$t \rightarrow c\gamma$	$4.6 \times 10^{-14}$	$7.5 \times 10^{-9}$	$\sim 10^{-6}$	$\sim 10^{-9}$	$2 \times 10^{-6}$	$1 \times 10^{-6}$
$t \rightarrow cg$	$4.6 \times 10^{-12}$	$1.5 \times 10^{-7}$	$\sim 10^{-4}$	$\sim 10^{-8}$	$8 \times 10^{-5}$	$2 \times 10^{-4}$
$t \rightarrow cH$	$3 \times 10^{-15}$	$4.1 \times 10^{-5}$	$1.5 \times 10^{-3}$	$\sim 10^{-5}$	$10^{-5}$	$\sim 10^{-6}$

Table 1: Branching ratios for top FCN decays in the SM, models with  $Q = 2/3$  quark singlets (QS), a general 2HDM, a flavour-conserving (FC) 2HDM, in the MSSM and with  $R$  parity violating SUSY.

## 4 Experimental observation

Present experimental limits on top FCN couplings come from the non-observation of the decays  $t \rightarrow qZ$ ,  $t \rightarrow q\gamma$  at Tevatron and the absence of single top production

$e^+e^- \rightarrow t\bar{q}$  at LEP and  $eu \rightarrow et$  at HERA. The best limits are  $\text{Br}(t \rightarrow qZ) \leq 0.159$  [21],  $\text{Br}(t \rightarrow q\gamma) \leq 0.032$  [22],  $\text{Br}(t \rightarrow u\gamma) \leq 0.011$  [23, 24] with a 95% confidence level (CL), very weak if compared to the rates which can be achieved in the SM and its extensions.<sup>1</sup> These limits will improve with Tevatron Run II, and will reach the  $10^{-5}$  level at LHC and TESLA (or other future  $e^+e^-$  collider), opening the possibility of the experimental observation of top FCN interactions.

## 4.1 Observation at LHC

At LHC top quarks are abundantly produced in  $t\bar{t}$  pairs via standard QCD interactions, with a cross section around 860 pb [1]. The search for top FCN couplings can be performed looking for processes in which the top quark decays via  $t \rightarrow qZ$  [25],  $t \rightarrow q\gamma$  [26],  $t \rightarrow qg$  [27],  $t \rightarrow qH$  [28], mediated by the operators in Eq. (1), while the antitop decays  $\bar{t} \rightarrow W^- \bar{b}$ . The charge conjugate processes, with standard top decay and FCN antitop decay, are also included in the analyses but for brevity we do not refer to them in the following. Due to the large QCD backgrounds at LHC, the search for signatures of these processes must be performed in the leptonic channels  $W^- \rightarrow \ell^- \bar{\nu}_\ell$ , with  $\ell = e, \nu$  (with a good  $\tau$  tagging this channel could be eventually included as well). In  $Z$  and  $H$  decays the channels considered are  $Z \rightarrow \ell^+ \ell^-$  and  $H \rightarrow b\bar{b}$ , respectively.  $b$  tagging is used in order to reduce backgrounds.

On the other hand, one can search for single top production mediated by the anomalous vertices in Eq. (1), in the processes  $gq \rightarrow Zt$  [29],  $gq \rightarrow \gamma t$  [29],  $gq \rightarrow t$  [30],  $gq \rightarrow Ht$  [28], followed by a standard top decay  $t \rightarrow W^+ b$ . The Feynman diagrams for these processes are depicted in Fig. 3.  $Zt$  and  $\gamma t$  production can also occur via  $gtq$  interactions, but the presence of this type of operator is easier to detect in the process  $gq \rightarrow t$ . We collect in Table 2 the tree-level cross sections for FCN single top production processes, calculated with MRST parton distribution functions set A [31]. Next-to-leading order corrections for  $Zt$  and  $\gamma t$  production are available for Tevatron energies [32]. For LHC they are expected to increase the cross sections at the 10% level.

It is clearly seen that for  $q = c$  these processes are suppressed by the smaller

---

<sup>1</sup>Our LEP bound on  $\text{Br}(t \rightarrow qZ)$  slightly differs from the one quoted in Ref. [21] because we normalise the rates to  $\Gamma(t \rightarrow bW^+)$ . The translation into limits on  $X_{qt}$  is also different from theirs, because they assume  $X_{ut} = X_{ct}$  while we assume only one coupling is different from zero, thus obtaining more conservative bounds.



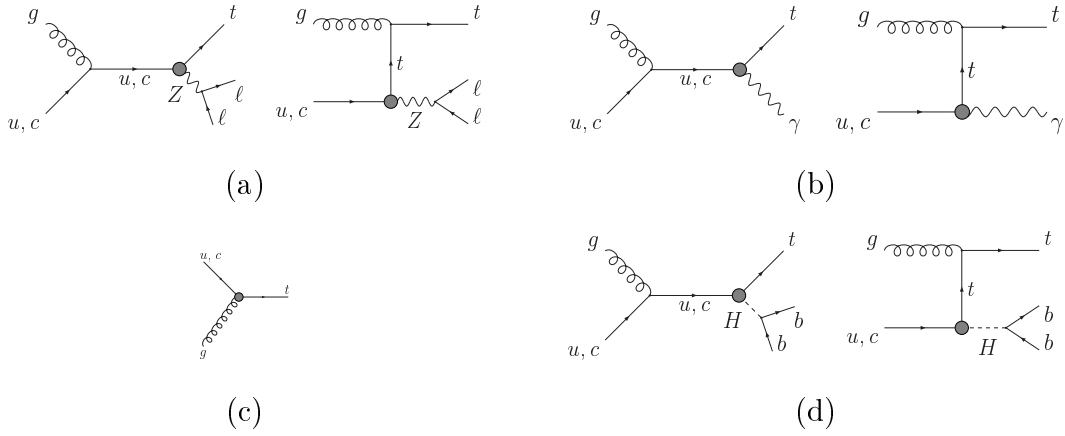


Figure 3: Diagrams for single top production in hadron collisions: (a)  $Zt$  production mediated by  $Ztq$  couplings; (b)  $\gamma t$  production mediated by  $\gamma tq$  couplings; (c)  $t$  production; (d)  $Ht$  production.

Process	Cross section	Process	Cross section
$gu \rightarrow Zt (\gamma_\mu)$	$(260 + 50)  X_{ut} ^2$	$gc \rightarrow Zt (\gamma_\mu)$	$(26 + 26)  X_{ct} ^2$
$gu \rightarrow Zt (\sigma_{\mu\nu})$	$(540 + 87)  \kappa_{ut} ^2$	$gc \rightarrow Zt (\sigma_{\mu\nu})$	$(45 + 45)  \kappa_{ct} ^2$
$gu \rightarrow \gamma t$	$(440 + 76)  \lambda_{ut} ^2$	$gc \rightarrow \gamma t$	$(39 + 39)  \lambda_{ct} ^2$
$gu \rightarrow t$	$(9.0 + 2.6) \times 10^5  \zeta_{ut} ^2$	$gc \rightarrow t$	$(1.5 + 1.5) \times 10^5  \zeta_{ct} ^2$
$gu \rightarrow Ht$	$(16 + 2.8)  g_{ut} ^2$	$gc \rightarrow Ht$	$(1.5 + 1.5)  g_{ct} ^2$

Table 2: Cross sections (in pb) for single top plus antitop production processes at LHC. In each case the first term in the sum corresponds to the process quoted and the second term to the charge conjugate process.

structure functions for the charm quark. For nonrenormalisable  $\sigma_{\mu\nu}$  couplings the cross sections are enhanced by the  $q^\nu$  factor appearing in the vertex: with the normalisation chosen for the coupling constants, for  $|X_{qt}| \simeq |\kappa_{qt}| \simeq |\lambda_{qt}|$  the first three branching ratios in Eq. (4) take similar values, while the cross sections in Table 2 are much larger for  $\sigma_{\mu\nu}$ -type interactions.

The search for these processes is cleaner in the channels where  $W^+ \rightarrow \ell^+ \nu_\ell$ ,  $Z \rightarrow \ell^+ \ell^-$ ,  $H \rightarrow b\bar{b}$ , and taking advantage of  $b$  tagging to reduce backgrounds. Their experimental signatures are written in Table 3, where we also include the most important backgrounds.

Process	Signal	Background		Process	Signal	Background	
$t\bar{t}, t \rightarrow qZ$	$\ell^+\ell^-j\ell\nu b$	$ZWjj$	LO	$gq \rightarrow Zt$	$\ell^+\ell^-\ell\nu b$	$ZWj$	LO
$t\bar{t}, t \rightarrow q\gamma$	$\gamma j\ell\nu b$	$\gamma Wjj$	LO**	$gq \rightarrow \gamma t$	$\gamma\ell\nu b$	$\gamma Wj$	LO
$t\bar{t}, t \rightarrow qq$	$j\bar{j}\ell\nu b$	$Wjjj$	LO*	$gq \rightarrow t$	$\ell\nu b$	$Wj$	NLO**
$t\bar{t}, t \rightarrow qH$	$b\bar{b}j\ell\nu b$	$Wb\bar{b}jj$	LO*	$gq \rightarrow Ht$	$b\bar{b}\ell\nu b$	$t\bar{t}$	NLO**

Table 3: Experimental signature and main background for several top rare decay and single top production processes at LHC. The top antiquarks are assumed to decay  $\bar{t} \rightarrow W^- \bar{b} \rightarrow \ell^- \bar{\nu}_\ell \bar{b}$ , and the  $Z$  and  $H$  bosons in the channel  $Z \rightarrow \ell^+\ell^-$ ,  $H \rightarrow b\bar{b}$ .

In order to determine the discovery potential of these processes we consider that only one FCN coupling  $X_{qt}$ ,  $\kappa_{qt}$ ,  $\lambda_{qt}$ ,  $\zeta_{qt}$  or  $g_{qt}$  is nonzero at a time. We give the limits for  $3\sigma$  evidence, what happens when the expected number of signal ( $S$ ) plus SM background ( $B$ ) events is not consistent with a background fluctuation at the  $3\sigma$  level, corresponding to a CL of 0.9973. For large samples, this translates into  $S/\sqrt{B} = 3$ , while for  $B \leq 5$  events Poisson statistics must be used. We rescale the data in Refs. [25, 26, 28–30] to a common  $b$  tagging efficiency of 50% and a mistagging rate of 1%, recalculating the limits using these unified criteria.<sup>2</sup> (We note that in these analyses a top quark mass  $m_t \simeq 175$  GeV is used.) We assume an integrated luminosity of  $100 \text{ fb}^{-1}$ , corresponding to one year of running in the high luminosity phase. For an increase in luminosity by a factor  $k$ , the limits on branching ratios scale with  $k^{-1/2}$ .

We point out that in real experiments a proper consideration of theoretical uncertainties in background cross sections will be compulsory. Present calculations in the literature are aimed at determining the sensitivity to FCN couplings of various processes, and do not need to take them into account. However, for the comparison of theoretical predictions with experimental data, leading order (LO) background calculations will often be insufficient and next-to-leading order (NLO) calculations will be required to match the statistical precision achieved at LHC. In Table 3 we have written the order in perturbation theory to which these backgrounds are presently known. We estimate that when the statistical uncertainty of the background cross sections<sup>3</sup> is better than 20% the use of NLO calculations is necessary (this is indicated in Table 3 by

<sup>2</sup>In Ref. [25]  $b$  tagging is not used and to obtain our limits we scale their cross sections by the appropriate factors. The interactions considered there are of  $\gamma_\mu$  type only but the limits for  $\sigma_{\mu\nu}$  couplings are expected to be the same. In Ref. [27] the analysis is done for Tevatron energies only.

<sup>3</sup>Including  $b$  tagging and kinematical cuts, and considering  $100 \text{ fb}^{-1}$  of integrated luminosity. For a higher luminosity the relative statistical uncertainty decreases.

an asterisk) and when it is better than 5%, next-to-next-to-leading-order calculations may be required (indicated by a double asterisk).<sup>4</sup>

Our limits are collected in Table 4. In the majority of the cases top decay processes provide the best place to discover top FCN interactions, surpassed by single top production for  $\sigma_{\mu\nu}$ -type interactions involving the up quark. Comparing these limits with the data in Table 1 we observe that in many examples the maximum rates predicted are observable with  $3\sigma$  statistical significance or more within one year (with a luminosity upgrade to  $6000 \text{ fb}^{-1}$  [33] the figures in Table 4 are reduced by a factor of 7.7). If no signal is observed, upper bounds on top FCN decay branching ratios can be placed. The 95% upper limits obtained in this case are numerically smaller than those in Table 4 by a factor between 1.3 and 1.5.

	Top decay	Single top		Top decay	Single top
$t \rightarrow uZ(\gamma_\mu)$	$3.6 \times 10^{-5}$	$8.0 \times 10^{-5}$	$t \rightarrow cZ(\gamma_\mu)$	$3.6 \times 10^{-5}$	$3.9 \times 10^{-4}$
$t \rightarrow uZ(\sigma_{\mu\nu})$	$3.6 \times 10^{-5}$	$2.3 \times 10^{-5}$	$t \rightarrow cZ(\sigma_{\mu\nu})$	$3.6 \times 10^{-5}$	$1.4 \times 10^{-4}$
$t \rightarrow u\gamma$	$1.2 \times 10^{-5}$	$3.1 \times 10^{-6}$	$t \rightarrow c\gamma$	$1.2 \times 10^{-5}$	$2.8 \times 10^{-5}$
$t \rightarrow ug$	—	$2.5 \times 10^{-6}$	$t \rightarrow cg$	—	$1.6 \times 10^{-5}$
$t \rightarrow uH$	$5.8 \times 10^{-5}$	$5.1 \times 10^{-4}$	$t \rightarrow cH$	$5.8 \times 10^{-5}$	$2.6 \times 10^{-3}$

Table 4:  $3\sigma$  discovery limits for top FCN interactions at LHC, for an integrated luminosity of  $100 \text{ fb}^{-1}$ . The limits are expressed in terms of top decay branching ratios.

The ATLAS and CMS collaborations have performed full detector simulations to investigate the sensitivity to the decays  $t \rightarrow qZ$ ,  $t \rightarrow q\gamma$ , giving  $5\sigma$  discovery limits on the rates for these processes for an integrated luminosity of  $100 \text{ fb}^{-1}$ . For the ATLAS detector the limits are  $\text{Br}(t \rightarrow qZ) = 2.0 \times 10^{-4}$  [34],  $\text{Br}(t \rightarrow q\gamma) = 1.0 \times 10^{-4}$  [1], and for the CMS detector  $\text{Br}(t \rightarrow qZ) = 1.9 \times 10^{-4}$ ,  $\text{Br}(t \rightarrow q\gamma) = 3.4 \times 10^{-5}$  [1]. After correcting for the different confidence levels used, the numbers for  $t \rightarrow q\gamma$  at CMS agree very well with those in Table 4, while the rest are more pessimistic.

To conclude this subsection we note that at LHC there are additional processes which can occur through top FCN interactions. The first example is single top production associated with a jet produced via  $gtq$  interactions [35], which is however less sensitive than  $gq \rightarrow t$ . The second example is like-sign top production [36], mediated

<sup>4</sup>In principle, it may be also possible to normalise the background cross sections using measured data from other phase space regions, thus decreasing the theoretical uncertainty in the regions of interest. If this is the case, NLO or even LO calculations may be sufficient.

by two FCN vertices. This process has a smaller cross section than processes with only one FCN vertex, but might be observed at LHC due to its small background.

## 4.2 Observation at an $e^+e^-$ collider

A high energy  $e^+e^-$  collider like TESLA will complement LHC capabilities in the search for top FCN couplings. As in hadron collisions, the operators in Eq. (1) mainly manifest themselves in top decay and single top production processes. In  $e^+e^-$  annihilation top quark pairs are produced by electroweak interactions, and single top quarks may be produced in the process  $e^+e^- \rightarrow t\bar{q}$ , [37], via the diagrams in Fig. 4. (The charge conjugate process is also summed.) At TESLA the top pair production cross section at 500 GeV is only of 600 fb [2], and limits obtained from top decays [38, 40] cannot compete with those from LHC, despite the larger luminosity and smaller backgrounds. On the contrary, single top production can match or even improve some LHC limits if beam polarisation is used to reduce backgrounds [39]. We have updated the study of Ref. [39] to include the effect of initial state radiation (ISR) [41] and beamstrahlung [42, 43] in the calculations. We assume integrated luminosities of  $345 \text{ fb}^{-1}$  and  $534 \text{ fb}^{-1}$  per year for centre of mass (CM) energies of 500 and 800 GeV, respectively [44], and beam polarisations  $P_{e^-} = 0.8$ ,  $P_{e^+} = -0.6$ .<sup>5</sup> For beamstrahlung at 500 GeV we use the parameters  $\Upsilon = 0.05$ ,  $N = 1.56$ , while at 800 GeV we take  $\Upsilon = 0.09$ ,  $N = 1.51$  [44]. We also include a beam energy spread of 1%. The total cross sections at both energies for each type of anomalous coupling are written in Table 5.

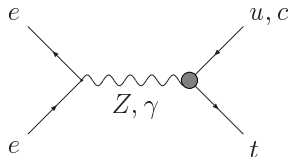


Figure 4: Diagrams for single top production in  $e^+e^-$  collisions.

We find that ISR and beamstrahlung make it more involved the reconstruction of the top quark momentum and additionally they increase the  $Wjj$  background cross section. Following the analysis of Ref. [39], but with a different reconstruction procedure and different sets of kinematical cuts, we obtain the  $3\sigma$  discovery limits in Table 6. The

---

<sup>5</sup>Here we use the convention in which the degree of polarisation refers to the helicity both for the electron and the positron, in contrast with Refs. [38, 39].

	500 GeV	800 GeV
$Z, \gamma_\mu$	$370  X_{qt} ^2$	$230  X_{qt} ^2$
$Z, \sigma_{\mu\nu}$	$2560  \kappa_{qt} ^2$	$2850  \kappa_{qt} ^2$
$\gamma$	$5370  \lambda_{qt} ^2$	$6300  \lambda_{qt} ^2$

Table 5: Cross sections (in fb) for single top production at TESLA, including ISR, beamstrahlung and beam energy spread, for polarisations  $P_{e^-} = 0.8$ ,  $P_{e^+} = -0.6$ . The cross section for single antitop production is the same.

limits for  $\gamma_\mu$  couplings to the  $Z$  boson are slightly better than the ones previously obtained in Ref. [39] without ISR and beamstrahlung, but still not competitive with those from LHC. For  $\sigma_{\mu\nu}$  interactions the opposite happens: limits including these corrections are a little worse but at any rate they improve the LHC potential in most cases, especially at 800 GeV, where the  $q^\nu$  factor in the vertex keeps signal cross sections large.

	500 GeV	800 GeV
$t \rightarrow qZ(\gamma_\mu)$	$1.9 \times 10^{-4}$	$1.9 \times 10^{-4}$
$t \rightarrow qZ(\sigma_{\mu\nu})$	$1.8 \times 10^{-5}$	$7.2 \times 10^{-6}$
$t \rightarrow q\gamma$	$1.0 \times 10^{-5}$	$3.8 \times 10^{-6}$

Table 6:  $3\sigma$  discovery limits for top FCN interactions in single top production at TESLA, for CM energies of 500 and 800 GeV, with respective luminosities of  $345 \text{ fb}^{-1}$  and  $534 \text{ fb}^{-1}$ . The limits are expressed in terms of top decay branching ratios.

We remark that LHC and TESLA are complementary in the search for top FCN interactions. LHC has a better discovery potential for  $\gamma_\mu$  couplings to the  $Z$  boson and FCN interactions with the gluon and the Higgs boson, while TESLA is more sensitive to  $\sigma_{\mu\nu}$  couplings to the  $Z$  and the photon. Moreover, if positive signals are observed, results from both colliders may be necessary to determine the type of operator involved. While TESLA cannot disentangle  $Z$  and photon interactions, its good  $c$  tagging efficiency may allow to determine the identity of the light quark. On the contrary, the processes described at LHC determine if the FCN vertices involve the  $Z$  boson or the photon, but it is more difficult to tag the flavour of the light quark.

### 4.3 Other colliders

For completeness, we list here other possible places where top FCN interactions can be probed as well. One possibility is  $e\gamma$  and  $\gamma\gamma$  collisions. The latter is specially sensitive, and a positive signal could be found in the context of the MSSM [45,46]. Note however that in this case there are further contributions to  $\gamma\gamma \rightarrow t\bar{c}$  given by box diagrams which cannot be parameterised by the vertices in  $\mathcal{L}^{\text{eff}}$ . (This is also the case for  $e^+e^-$  annihilation [47].)  $ep$  scattering is another place where this type of interactions might lead to new effects, but their sensitivity is far beyond the ones achievable at LHC or a future  $e^+e^-$  collider.

## 5 Conclusions

In the previous sections we have seen that top FCN couplings are negligible in the SM but can be enhanced in SM extensions. We have shown that these interactions lead to observable effects at high energy colliders, mainly in top decay and single top production processes. In order to cleanly observe an excess with respect to SM expectations, and hence the presence of top FCN interactions, a precise background calculation is compulsory. This is a task which should be carried out in the next few years, before LHC experimental data are available.

We have shown that top FCN interactions offer a good place for the study of indirect effects from physics beyond the SM. However, one important aspect which has not been discussed is the correlation between top FCN processes and other possible new physics effects at high or low energies. This study includes, but is not limited to, the effect of top FCN operators in low energy physics [48]. Although the branching ratios in Table 1 are in agreement with present experimental data, effects in  $B$  physics are possible and could be measured in experiments under way at  $B$  factories.

One example of such correlation is present in models with  $Q = 2/3$  singlets. A coupling  $|X_{ct}| \sim 0.015$  observable at LHC requires a sizeable deviation of the diagonal  $Ztt$  coupling from its SM expectation [7], which would certainly be seen in  $t\bar{t}$  production at TESLA. Furthermore, a FCN coupling of this size allows for a CP-violating phase  $\chi = \arg(V_{ts}V_{tb}^*V_{cs}^*V_{cb}) \sim \pm 0.3$  in the CKM matrix [49], much larger in absolute value than the SM expectation  $0.015 \leq \chi \leq 0.022$ . This phase would lead to observable phenomena in  $B$  oscillations and decay and, if such a phase is found, it necessarily requires the presence of a FCN coupling at the observable level.

The examination of possible correlations between top FCN interactions and other processes at low and high energies is model-dependent, and further analyses should be done in that direction. In particular, if indirect effects are meant to serve as consistency tests of a (new physics) model, the relation between the presence of top FCN interactions at an observable level and other indirect effects must be fully understood. The investigation of such correlations will help uncover the nature of new physics, if positive signals are found at the present or next generation of colliders.

## Acknowledgements

I thank F. del Águila for discussions. This work has been supported by the European Community's Human Potential Programme under contract HTRN-CT-2000-00149 Physics at Colliders and by FCT through projects CERN/FIS/43793/2002, CFIF-Plurianual (2/91) and grant SFRH/BPD/12603/2003.

## References

- [1] M. Beneke *et al.*, hep-ph/0003033
- [2] J. A. Aguilar-Saavedra *et al.* [ECFA/DESY LC Physics Working Group Collaboration], hep-ph/0106315
- [3] P. Azzi *et al.* [CDF and D0 Collaborations and Tevatron Electroweak Working Group], hep-ex/0404010
- [4] G. Eilam, J. L. Hewett and A. Soni, Phys. Rev. D **44** (1991) 1473 [Erratum-ibid. D **59** (1999) 039901]
- [5] B. Mele, S. Petrarca and A. Soddu, Phys. Lett. B **435** (1998) 401
- [6] J. A. Aguilar-Saavedra and B. M. Nobre, Phys. Lett. B **553** (2003) 251
- [7] J. A. Aguilar-Saavedra, Phys. Rev. D **67** (2003) 035003 [Erratum-ibid. D **69** (2004) 099901]
- [8] F. del Águila, J. A. Aguilar-Saavedra and R. Miquel, Phys. Rev. Lett. **82** (1999) 1628

- [9] T. P. Cheng and M. Sher, Phys. Rev. D **35** (1987) 3484
- [10] M. E. Luke and M. J. Savage, Phys. Lett. B **307** (1993) 387
- [11] D. Atwood, L. Reina and A. Soni, Phys. Rev. D **55** (1997) 3156
- [12] S. Bejar, J. Guasch and J. Sola, Nucl. Phys. B **600** (2001) 21
- [13] J. J. Liu, C. S. Li, L. L. Yang and L. G. Jin, Phys. Lett. B **599** (2004) 92
- [14] D. Delepine and S. Khalil, Phys. Lett. B **599** (2004) 62
- [15] C. S. Li, R. J. Oakes and J. M. Yang, Phys. Rev. D **49** (1994) 293 [Erratum-ibid. D **56** (1997) 3156]
- [16] G. M. de Divitiis, R. Petronzio and L. Silvestrini, Nucl. Phys. B **504** (1997) 45
- [17] J. L. Lopez, D. V. Nanopoulos and R. Rangarajan, Phys. Rev. D **56** (1997) 3100
- [18] J. Guasch and J. Sola, Nucl. Phys. B **562** (1999) 3
- [19] J. M. Yang, B. L. Young and X. Zhang, Phys. Rev. D **58** (1998) 055001
- [20] G. Eilam, A. Gemintern, T. Han, J. M. Yang and X. Zhang, Phys. Lett. B **510** (2001) 227
- [21] G. Abbiendi *et al.* [OPAL Collaboration], Phys. Lett. **B521** (2001) 181
- [22] F. Abe *et al.* [CDF Collaboration], Phys. Rev. Lett. **80** (1998) 2525
- [23] S. Chekanov *et al.* [ZEUS Collaboration], Phys. Lett. B **559** (2003) 153
- [24] A. Aktas *et al.* [H1 Collaboration] Eur. Phys. J. C **33** (2004) 9
- [25] T. Han, R. D. Peccei and X. Zhang, Nucl. Phys. B **454** (1995) 527
- [26] T. Han, K. Whisnant, B. L. Young and X. Zhang, Phys. Rev. D **55** (1997) 7241
- [27] T. Han, K. Whisnant, B. L. Young and X. Zhang, Phys. Lett. B **385** (1996) 311
- [28] J. A. Aguilar-Saavedra and G. C. Branco, Phys. Lett. B **495** (2000) 347
- [29] F. del Aguila and J. A. Aguilar-Saavedra, Nucl. Phys. B **576** (2000) 56
- [30] M. Hosch, K. Whisnant and B. L. Young, Phys. Rev. D **56** (1997) 5725



- [31] A. D. Martin, R. G. Roberts, W. J. Stirling and R. S. Thorne, hep-ph/0307262
- [32] N. Kidonakis and A. Belyaev, JHEP **0312** (2003) 004
- [33] O. Bruning *et al.*, CERN-LHC-PROJECT-REPORT-626
- [34] L. Chikovani and T. Djobava, hep-ex/0205016
- [35] T. Han, M. Hosch, K. Whisnant, B. L. Young and X. Zhang, Phys. Rev. D **58** (1998) 073008
- [36] Y. P. Gouz and S. R. Slabospitsky, Phys. Lett. B **457** (1999) 177
- [37] T. Han and J. L. Hewett, Phys. Rev. **D60** (1999) 074015
- [38] J. A. Aguilar-Saavedra and T. Riemann, LC-TH-2001-067, hep-ph/0102197
- [39] J. A. Aguilar-Saavedra, Phys. Lett. **B502** (2001) 115
- [40] T. Han, J. Jiang and M. Sher, Phys. Lett. B **516** (2001) 337
- [41] M. Skrzypek and S. Jadach, Z. Phys. C **49** (1991) 577
- [42] K. Yokoya and P. Chen, SLAC-PUB-4935. *Presented at IEEE Particle Accelerator Conference, Chicago, Illinois, Mar 20-23, 1989*
- [43] M. Peskin, Linear Collider Collaboration Note LCC-0010, January 1999
- [44] International Linear Collider Technical Review Committee 2003 Report, <http://www.slac.stanford.edu/xorg/ilc-trc/2002/2002/report/03rep.htm>
- [45] J. j. Cao, Z. h. Xiong and J. M. Yang, Nucl. Phys. B **651** (2003) 87
- [46] J. M. Yang, Annals Phys. **316** (2005) 529
- [47] S. Bar-Shalom and J. Wudka, Phys. Rev. **D60** (1999) 094016
- [48] R. D. Peccei, S. Peris and X. Zhang, Nucl. Phys. B **349** (1991) 305
- [49] J. A. Aguilar-Saavedra, F. J. Botella, G. C. Branco and M. Nebot, Nucl. Phys. B **706** (2005) 204